CrossMark

Callosal microstructure affects the timing of electrophysiological left-right differences

Patrick Friedrich [a],[*],[1], Sebastian Ocklenburg [a],[1], Nina Heins [a], Caroline Schlüter [a], Christoph Fraenz [a], Christian Beste [b],[c], Onur Güntürkün [a], Erhan Genç [a]

[a] Institute of Cognitive Neuroscience, Biopsychology, Department of Psychology, Ruhr-University of Bochum, Germany
[b] Cognitive Neurophysiology, Department of Child and Adolescent Psychiatry, Faculty of Medicine of the TU Dresden, Germany
[c] Experimental Neurobiology, National Institute of Mental Health, Klecany, Czech Republic

ARTICLE INFO

ABSTRACT

The neural architecture of the corpus callosum shows pronounced inter-individual differences. These differences are thought to affect timing of interhemispheric interactions and, in turn, functional hemispheric asymmetries. The present study aimed at elucidating the neuronal mechanisms underlying this relationship. To this end, we used a combined DTI and EEG study design. In 103 right-handed and healthy adult participants, we determined the microstructural integrity of the posterior third of the corpus callosum and examined in how far this microstructural integrity was related to between-hemisphere timing differences in neurophysiological correlates of attentional processes in the dichotic listening task. The results show that microstructural integrity of the posterior callosal third correlated with attentional timing differences in a verbal dichotic listening condition but not in a noise control condition. Hence, this association between callosal microstructure and between-hemisphere timing differences is specific for stimuli, which trigger hemispheric bottom-up processing in an asymmetric fashion. Specifically, higher microstructural integrity was associated with decreased left-right differences in the latency of the N1 event-related potential component and hence more symmetric processing of dichotic stimuli between the two hemispheres. Our data suggest that microstructure of the posterior callosal third affects functional hemispheric asymmetries by modulating the timing of interhemispheric interactions.

1. Introduction

The corpus callosum is thought to be a fundamental factor for the emergence and maintenance of functional hemispheric asymmetries (Bryden and Bulman-Fleming, 1994; Ringo et al., 1994; Bamiou et al., 2007; Luders et al., 2010; Ocklenburg et al., 2016a). It is widely accepted to play an important role in both the integration and modulation of various processes in favor of the dominant hemisphere (Bloom and Hynd, 2005). One of the arguments for this role is the conduction velocity of callosal fibers, which can be estimated from their myelination and diameter. Electron microscopic studies indicate that in monkeys the majority of callosal axons are unmyelinated and have an average diameter of 0.75 μm (Lamantia and Rakic, 1990). In adult humans axon diameter varies between 0.6 and 1.0 μm (Aboitiz et al., 1992) and around 70% of callosal fibers are myelinated (Fields, 2008). The myelination

influences the conduction time between the left and right hemispheres. In myelinated callosal fibers the conduction velocity is approximately 30 ms and between 150 and 300 ms in unmyelinated callosal fibers. Importantly, inter-individual variation of the callosal architecture in humans has been linked to the speed of interhemispheric processing (Westerhausen et al., 2006b; Horowitz et al., 2015) and callosal inter-action is important for the establishment of functional brain asymmetries (Gazzaniga, 2000; Herve et al., 2013). However, it is virtually unknown to what extent the callosal architecture mediates the speed of hemispheric processing in the context of functional hemispheric asymmetries.

A prominent example of functional hemispheric asymmetries is speech perception (Bethmann et al., 2007; Ocklenburg et al., 2013b; Van der Haegen et al., 2013; Hugdahl and Westerhausen, 2016), which can be demonstrated with the dichotic listening paradigm (DLT). In this simple task, two different consonant-vowel syllables are simultaneously

presented to the left and the right ear via headphones (Hugdahl, 2011), resulting in a larger number of correct reports from the right ear - the so-called „right ear advantage" (REA) (Foundas et al., 2006). Since left-hemispheric auditory areas mainly process input from the right ear, the REA is thought to reflect the extent of left-sided dominance for auditory speech perception. Interestingly, the strength of the REA shows large inter-individual variation (Hirnstein et al., 2014). With regards to the role of the corpus callosum for dichotic listening, two theoretical models have been proposed to explain the neural foundation of this inter-individual variance.

According to the "structural model" (Kimura, 1967, 2011), the REA is caused by the anatomy of the ascending auditory pathway. Since contralateral projections are stronger than ipsilateral projections, right ear input is processed in the speech dominant left hemisphere, while input from the left ear primarily arrives in the non-dominant right hemisphere. Therefore, left ear input needs to be transferred to the left hemisphere to be processed. This transfer process is thought to occur via the corpus callosum. According to the "attentional model" (Kinsbourne, 1970; Hiscock and Kinsbourne, 2011), the anticipation of verbal stimuli leads to a preparatory left-hemispheric activation, resulting in an attentional bias towards the right ear. Hence, the right ear input is processed faster, thus producing the REA. In this model, the corpus callosum is thought to equalize the level of activation between the two hemispheres. Importantly, both models make the same prediction about the influence of the corpus callosum on the REA: a higher structural integrity of the corpus callosum is thought to lead to a more symmetric performance, because of better interactive capacities between the two hemispheres.

Indeed, this relation has been examined in clinical studies and studies in healthy individuals on different anatomical levels. First, clinical studies support the role of the corpus callosum in dichotic listening, as partial or complete callosotomy leads to increased REA in favor of the left hemisphere, based on a suppression of left ear reports (Clarke et al., 1993; Pollmann et al., 2002; Peru et al., 2003; Musiek and Weihing, 2011). Hence, the absence of the corpus callosum leads to stronger functional hemispheric asymmetries. Second, macroscopic anatomical properties of the corpus callosum, like the size of the midsagittal area, are positively correlated with the percentage of correct left ear reports and negatively correlated with the percentage of correct right ear reports (Westerhausen et al., 2006c). Thus, callosal macrostructure is associated with less functional asymmetry between the two hemispheres. Yet, more recent imaging methods such as diffusion tensor imaging (DTI) allow in-vivo tractography of specific fiber tracts (Catani et al., 2002; Behrens et al., 2007) as well as the microstructural quantification via means of fractional anisotropy (FA) (Basser and Pierpaoli, 1996). FA in white matter is thought to reflect myelin, axon diameter and packing density, axon permeability and fiber geometry (Wedeen et al., 2005; Mori and Zhang, 2006; Madler et al., 2008; Beaulieu, 2009; Zatorre et al., 2012) and is thus seen as a measure of microstructural integrity (Schulte et al., 2005; Genc et al., 2011a; Van Schependom et al., 2017), which in turn is associated with conduction velocity. DTI examinations in humans show that fiber connections within the corpus callosum are arranged in a topographic manner (Hofer and Frahm, 2006; Zarei et al., 2006). Especially the posterior third of the corpus callosum consists of interhemispheric fibers connecting the temporal cortices with each other. The posterior callosal third is important for transmitting both syntactic and prosodic information (Sammler et al., 2010). Accordingly, Westerhausen et al. (2009) identified transcallosal fibers in the posterior parts of the corpus callosum, which interconnect the superior temporal regions of both hemispheres. They found that the mid-sagittal tract size of superior temporal projections was positively correlated with the percentage of correct left ear reports. However a link between correct left ear reports and callosal microstructure was not found. Similarly, the neurophysiological basis of this effect in relation to the callosal microstructure is elusive.

There is clear evidence that the N1 event-related potential (ERP) component for dichotic stimuli, reflecting bottom-up attentional

processes (Herrmann and Knight, 2001; Beste et al., 2010; Ocklenburg et al., 2012), is faster in the left than right the hemisphere; i.e. there is a strong latency difference between the hemispheres (Eichele et al., 2005). Since the important link between electrophysiological timing differences and callosal microstructure has not been shown so far, the current study examines this aspect by means of a dichotic listening task. The study is the first that interrelates electrophysiology and callosal microstructure. Given the evidence of a link between callosal microstructure and conduction velocity, we hypothesized that hemispheric latency difference is decreased in participants with higher microstructural integrity of the posterior callosal third.

2. Methods

2.1. Subjects

145 German-speaking volunteers (68 males and 77 females) with a mean age of 23.5 years (range 18–33) participated in the present study. We used the Edinburgh Handedness Inventory (EHI) to examine the handedness for each participant (Oldfield, 1971). This questionnaire yields a laterality quotient with a range between +100 and −100, with positive values indicating right- and negative values indicating left-handedness. The sample consisted of 106 right-handed (mean laterality quotient: 85.88, SD: 20.32) and 39 left-handed participants (mean laterality quotient: −73.39, SD: 24.89). All participants were healthy with no history of psychiatric or neurological disorders. Before the experiment, all participants underwent audiometric screening. None of the participants included in our final sample had interaural differences above 15 dB for any of the tested frequencies (6000 Hz, 3000 Hz, 1500 Hz and 750 Hz). Participants were given written informed consent and were either paid or compensated with course credit. Due to difficulties with the EEG acquisition, four participants (2 males and 2 females, 1 left-handed and 3 right-handed) were excluded from the study. Thus the final sample consisted of 141 participants (67 males, 38 left-handed). The right-handed subsample (n = 103; 48 males) showed a mean age of 23.7 years (range 19–33) and the averaged EHI laterality quotient was 85.99 (SD = 20.15). The left-handed subsample (n = 38; 19 males) had a mean age of 22.84 (SD = 3.03) and an averaged EHI laterality quotient of −72.69 (SD = 24.83). The ethics committee of the psychological faculty at Ruhr-University Bochum approved the study. All participants gave written informed consent and were treated in accordance with the declaration of Helsinki. Subjects were tested in two sessions. The first session included the handedness questionnaire and the EEG dichotic listening task. The second session consisted of the MRI imaging.

2.2. Dichotic listening paradigm

At the beginning of the experiment participants were seated in a chair in front of the presentation monitor, while EEG electrodes were already attached to the participant's scalp. The experiment was a passive dichotic listening task, which was conducted in accordance with a previous study (Beste et al., 2015). The stimuli consisted of six different consonant-vowel syllable pairs (e.g., "BA, "DA", "GA", "KA", "PA", and "TA") that were digitally recorded and spoken by an adult German male. These stimuli were pretested and validated in previous studies (Ocklenburg et al., 2013a). Stimulus presentation was conducted using Presentation software (Neurobehavioural Systems, Inc., Albany, USA) at 30 dB via earphones. Participants were instructed to passively listen to the presented sounds. Differences between the voice onset times of voiceless ("KA", "PA", and "TA") and voiced consonants ("BA", "DA" and "GA") were controlled for, thus the temporal envelopes of the syllables were matched. In the "dichotic condition" two different syllables were presented simultaneously to the two ears. All possible syllable pairs were presented counterbalanced to both ears, to avoid possible confounding effects of syllable-type. A "noise condition" was included as a control measure, in which the participants were confronted with white noise on

both ears instead of syllables. The experiment started with a training block presenting 10 trials to familiarize the participants with the different sounds. Subsequently, three experimental blocks were conducted without pause. Within each block, 30 dichotic trials and 30 noise trials were presented, making a total of 180 trials with 90 trials for each condition. The noise trials were included as a control condition to ensure the testing of specific lateralization effects, rather than a general auditory phenomenon. The order of stimuli was randomized, with stimulus duration of 350 ms for each trial. To avoid stimulus habituation effects, inter-stimulus interval was jittered between 3150 and 3650 ms.

2.3. EEG recording and analysis

EEG signals during the passive dichotic listening task were recorded with a 64 Ag/AgCl electrode grid (actiCAP ControlBox and QuickAmp 72, Brain Products, GmbH, Gilching Germany) from standard scalp positions. Data was recorded with a sampling rate of 1,000 Hz with FCz as reference electrode. The impedance of all electrodes was below 5 kΩ. For further processing of the raw data, we used Brain Vision Analyser II software (Brain Products GmbH). First, the signal was filtered with a band pass (IIR)-filter between 0.5 and 20 Hz, before we visually inspected the EEG data to identify technical artifacts. If a channel showed clear artifacts, it was removed from the following analysis. To identify systematic artifacts caused by blinks, eye movements or pulse, an independent component analysis (ICA) applying the infomax algorithm was used. ICA-components that reflected these artifacts were excluded. Subsequently, previously excluded channels as well as FCz were interpolated topographically with spherical splines, on basis of the surrounding electrodes. For each condition, separate segments were created starting from −100 ms before and ended 500 ms after stimulus presentation. Afterwards, an automated artifact rejection procedure was applied for each segment using the following criteria: maximal amplitude difference of 200 (μV) in a 100-ms interval as well as an activity below 0.5 (μV) in a 200 ms period as rejection criteria. Thus, if a rejection criterion was reached for any electrode, the whole segment was excluded from further analysis. Less than 1% of the trials were rejected by this method. After baseline correction from −100ms to time point zero, the signal was averaged for each channel. For subsequent N1 peak detection, we chose the electrode positions C5 and C6, which have shown to produce strong and reliable N1 responses in DLT (Beste et al., 2015) and auditory stimuli in general using that particular electrode setup (Muckschel et al., 2014). Furthermore, scalp topography plots as well as visual peak inspections validated this choice (see result section and Fig. 3). Hence, N1 ERP components were identified for these two electrodes. We used a semi-automatic local peak detection algorithm implemented in Brain-VisionAnalyzer, to identify N1. Based on earlier findings (Eichele et al., 2005; Beste et al., 2015), N1 was measured as the most negative peak in a time window from 70 to 180 ms after stimulus presentation. All peaks were visually inspected and changed occasionally, in cases were the algorithm missed the peak. Less then 5% of peaks were adjusted. Afterwards, the amplitude and latency of the N1 peak was extracted for the left (C5) and right (C6) electrodes for further analyses. Finally, the latency difference (LD) was calculated by subtracting N1 peak onset of the left electrode from N1 peak onset of the right one, indicating that a positive LD value reflects an earlier left hemispheric N1 peak onset compared to the right hemispheric N1 peak onset.

2.4. sLORETA analysis

We used sLORETA (standardized low resolution brain electromagnetic tomography) to reconstruct the cortical distribution of source locations contributing to the N1 ERP component during dichotic listening. sLORETA (Pascual-Marqui, 2002) is a improved version of the previously developed LORETA (Pascual-Marqui et al., 1994) and provides a single linear solution to the inverse problem of localizing the sources of brain functions without localization bias (Greenblatt et al., 2005; Sekihara

et al., 2005). The localization accuracy has been validated by several studies using simultaneous EEG/fMRI (Mulert et al., 2004; Olbrich et al., 2009) as well as TMS/EEG studies (Dippel and Beste, 2015; Gohil et al., 2016). A three-dimensional head model of the MNI152 template (Mazziotta et al., 2001) is used for visualization, partitioned in 6239 voxels at 5 mm spatial resolution. For each voxel, standardized current density is calculated. For the statistics the sLORETA-built-in voxel-wise randomization tests with 5000 permutations, based on statistical nonparametric mapping (SnPM) were performed. On the basis of the waveforms in the dichotic condition, we used the sLORETA-built one-sample t-test to examine the source of amplitudes. Voxels with significant difference from zero (p < 0.01, corrected for multiple comparisons) as well as coordinates in MNI space were determined using sLORETA viewer.

2.5. DTI imaging and analysis

First we acquired a T1-weighted high-resolution anatomical scan (MP-Rage, TR = 8179 ms, TE = 3.7 ms, flip angle = 8°, 22 slices, matrix size = 240 × 240, resolution = 1 × 1 × 1 mm), for co-registration of diffusion images. The total acquisition time for each of this scan was 6 min.

Three consecutive diffusion-weighted single-shot spin-echo echo-planar images were acquired afterwards. Diffusion weighting was isotropically distributed along 60 directions using a b-value of 1000 s/mm^2. Additionally, for motion correction and computation of diffusion co-efficients, ten data sets were acquired without diffusion weighting. To increase signal-to-noise ratio (Genc et al., 2011b; Genc et al., 2015), we averaged the three images as a first preprocessing step. For further analyses, we used FDT (FMRIB's Diffusion Toolbox), which is implemented in FSL (www.fmrib.ox.ac.uk/fsl). Preprocessing steps included the correction for eddy current and motion as well as volume-wise correction of the gradient direction using the rotation parameters from head motion. For the evaluation of microstructural integrity, we calculated fractional anisotropy (FA) maps via DTIFIT. By using FNIRT all diffusion images were non-linearly aligned to the standard space template of the MNI brain (FMRIB58_FA). In order to test whether the inter-individual variation of hemispheric differences in LD is related to the individual callosal white-matter microstructure we performed a standardized geometrical parcellation of the CC for all individuals. The parcellation schema proposed by Hofer and Frahm (2006) was utilized to identify the anterior callosal third, mid segment and posterior callosal third on the FMRIB58_FA_1mm template (see Fig. 1). The the posterior callosal third is thought to contain white-matter fibers from auditory cortices (Park et al., 2008; Westerhausen et al., 2009), whereas the anterior third and mid segment were used as control segments. Since FA images of all participants were non-linearly aligned to MNI standard space, we used an automatic procedure in transforming the callosal segments back to the raw diffusion space of the FA images for each participant. Finally, we computed for each participant the mean FA value of the posterior third, mid segment and anterior third. In addition, to assess FA values of the whole white matter, we performed an automated tissue parcellation using FreeSurfer (http://surfer.nmr.mgh.harvard.edu, version 5.3.0) on the individual T1-weighted images, to reconstruct gray and white matter tissue. The details of this procedure have been described elsewhere (Dale et al., 1999; Fischl et al., 1999). The automatic construction steps included skull stripping and gray and white matter segmentation. After preprocessing, segmentation was quality controlled slice-wise and inaccuracies for the automatic steps were corrected by manual editing if necessary. Brain segmentation yielded an estimate of overall white matter tissue. The resulting white matter mask was linearly transformed into the native space of the diffusion-weighted images to compute for each individual the mean FA value for the whole white matter.

2.6. Statistical analyses

Statistical analyses were performed using SPSS (version 20, SPSS Inc.,
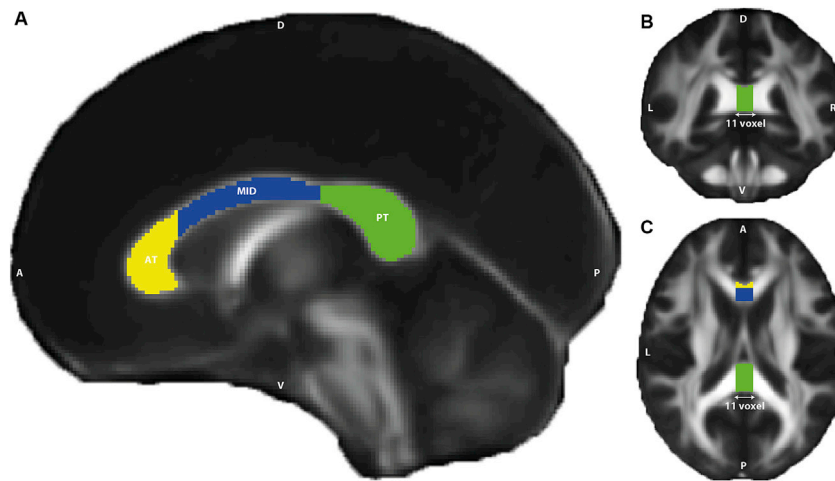
Fig. 1. Callosal segments used for analyzing the structure-function relation. The image is presented in (A) mid-sagittal view, (B) coronal view, and (C) on the diffusion space MNI FA image (FMRIB_FA_1 mm). Three callosal segments were created in accordance with the proposed scheme of Hofer and Frahm (2006). All three are visible in the mid-sagittal segment: AT = anterior third, MID = mid segment, PT = posterior third. Image directions are presented as follows: A = anterior, P = posterior, D = dorsal, V = ventral, L = left, R = right.

Chicago, IL, United States of America). For all analyses, we used linear parametric methods with an α-level of 0.05. To test if the latencies or amplitudes of the two hemispheres differ with regards to the experimental conditions, we conducted a two-way (2 × 2) repeated measure ANOVA with hemisphere (left; right) and condition (dichotic; noise) as within-participants factors. To test our hypothesis we calculated Pearson's correlation coefficient between LD and FA for both the noise and dichotic condition. Furthermore, to test for potential confounds and the specificity of our structure-function relationships we performed two multiple regression analysis with LD of the dichotic condition as independent variable. In the first multiple regression analysis we included FA values of the posterior callosal third and whole white matter as predictors. For the second multiple regression analysis we included FA values of the three callosal segments (posterior third, mid segment and anterior third) as predictors.

3. Results

3.1. Levene's test of variance homogeneity

Since our sample consists of an unequal number of left- and right-handed participants, we used Levene's test of variance homogeneity on the residuals of the standard error of N1 latency differences in the dichotic and noise condition. For latencies in both conditions, Levene's

test only missed significance by a small margin (dichotic: $F_{(1, 139)} = 3.48$, $p = 0.06$; noise: $F_{(1, 139)} = 3.23$, $p = 0.08$). Therefore, we decided to split the sample by handedness and report separate statistical tests for the left- and right-handed subsample.

3.2. EEG results – right-handers

We computed a two-way (2 × 2) repeated ANOVA with hemisphere (left, right) and condition (dichotic, noise) as within-subject factors, with N1 amplitude or N1 latency as dependent variable. For right-handed participants, the comparisons of amplitude and latencies between conditions are visualized in Fig. 2.

The ANOVA in amplitude of the right-handed subsample revealed a significant main effect of condition ($F_{(1, 102)} = 298.921$, $p < 0.001$, $\eta2_p = 0.75$), driven by higher N1 amplitude in the dichotic condition ($-2.52 \mu V \pm 0.12$) compared to lower N1 amplitude in the noise condition ($-0.49 \mu V \pm 0.68$). There was neither a significant main effect of hemisphere ($F_{(1, 102)} = 2.68$, $p = 0.11$, $\eta2_p = 0.03$) nor a significant interaction between hemisphere and condition ($F_{(1,102)} = 0.68$, $p = 0.41$, $\eta2_p < 0.01$).

For latencies, the ANOVA yielded a significant main effect of hemisphere ($F_{(1, 102)} = 23.40$, $p < 0.001$, $\eta2_p = 0.19$), driven by earlier N1 peak onsets in the left hemisphere (110.64 ms ± 1.31) compared to N1 peak onsets in the right hemisphere (119.37 ms ± 1.14). Also, a
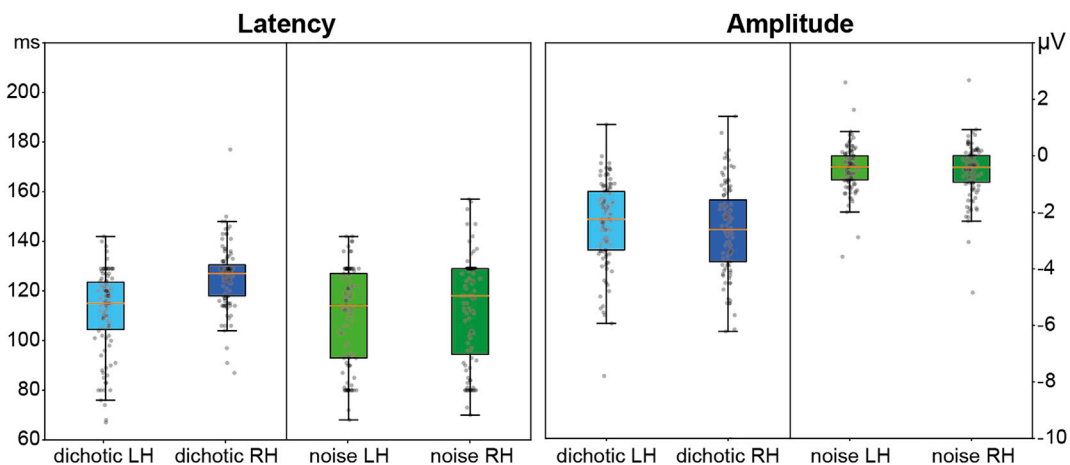
Fig. 2. Boxplots for right-handed subsample showing latencies and amplitudes of C5 and C6 electrode on the left hemisphere (LH) and right hemisphere (RH) respectively. Light and dark blue boxplots belong to the dichotic condition. Light and dark green boxplots belong to the noise condition. The scattered points represent single participants.

significant main effect of condition was found ($F_{(1, \ 102)} = 17.53$, $p < 0.001$, $\eta^2_p = 0.15$). Comparing conditions showed that averaged N1 peak onset was earlier in the noise condition (111.25 ms ± 1.33) than averaged N1 peak onset of the dichotic condition (118.75 ms, ± 1.10). Moreover, the interaction between hemisphere and condition was significant ($F_{(1, 102)} = 8.40$, $p < 0.01$, $\eta^2_p = 0.08$). Bonferroni corrected post-hoc test revealed that the interaction was driven by hemispheric differences in the dichotic condition ($p < 0.001$), with earlier N1 peak onset in the left hemisphere (111.77 ms ± 1.64) compared to N1 peak onset of the right hemisphere (125.72 ms ± 1.24). In contrast, there was no significant difference in N1 peak onset between the left hemisphere (109.49 ms ± 1.94) and right hemisphere (113.02 ms ± 2.10) in the noise condition ($p = 0.25$). The averaged EEG waveforms in the right-handed sample are illustrated in Fig. 3 for both the dichotic condition (3A) and noise condition (3B) for the chosen electrodes.

3.3. EEG results – left-handers

Similar to the right-handed subsample, we conducted a two-way (2 × 2) repeated ANOVA with hemisphere (left, right) and condition (dichotic, noise) as within-subject factors, with N1 amplitude or N1 latency as dependent variable. While the results of the ANOVA in amplitude were comparable to the analysis in right-handed participants, the ANOVA in latencies showed a different pattern of results. Similar to right-handers, the ANOVA in amplitude only revealed a significant main effect of condition ($F_{(1, 37)} = 86.40$, $p < 0.001$, $\eta^2_p = 0.70$; all other $p > 0.10$), caused by higher amplitudes in the dichotic condition (−2.53 ± 0.23) compared to the noise condition (−0.52, ±0.09).

For latencies, the ANOVA was not significant for the main effect of hemisphere ($F_{(1, \ 37)} = 2.01$, $p = 0.17$) or condition ($F_{(1, \ 37)} = 0.23$, $p = 0.23$). However, the interaction effect between hemisphere and condition ($F_{(1, 37)} = 6.41$, $p < 0.02$, $\eta^2_p = 0.15$) was significant, due to the
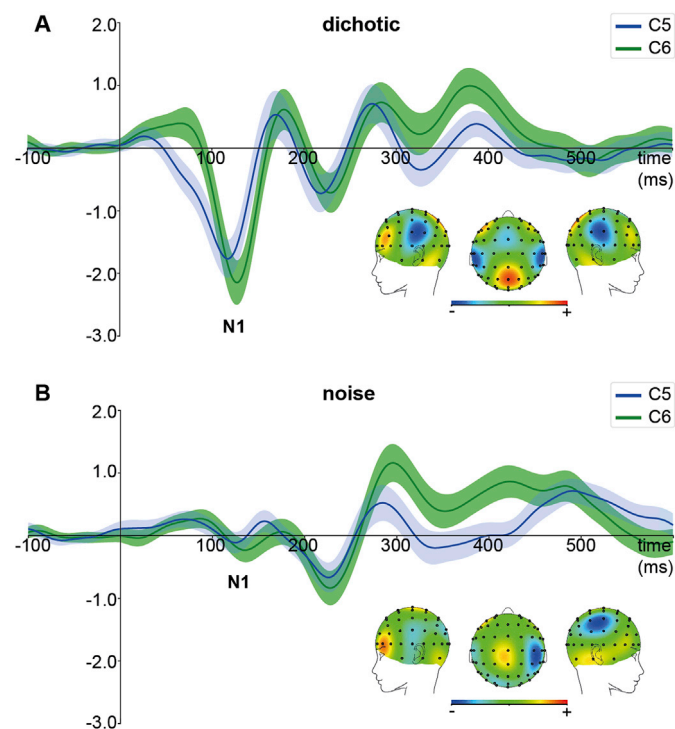
Fig. 3. A Averaged event-related potentials (ERPs) of dichotic listening stimuli for electrodes C5 and C6. Electrode C5 reflects stimuli presented to the right ear, whereas electrode C6 reflects stimuli presented to the left ear. The topographical map underlines the use of these two electrodes, as they strongly reflect the N1 in the dichotic condition. The scalp topography plots are color coded, with cold colors denoting negativity and warm colors denoting positivity. Error lines represent 95% confidence interval. **B** ERPs and topographical map for noise stimuli.

earlier N1 peak onset in the left hemisphere during dichotic condition compared to N1 peak onset in the right hemisphere (left: 111.82 ± 2.54; right: 123.61 ± 3.61; Bonferroni corrected *t*-test: $p < 0.05$). The comparison of amplitude and latencies between conditions in left-handed participants is visualized in Fig. S1.

Since left-handers did not show a significant main effect of condition in N1 latency, all following analyses were computed only for the right-handed subsample.

3.4. sLORETA results for dichotic condition

In order to reconstruct the cortical distribution of source locations contributing to the N1 ERP component we computed a sLORETA analysis for the right-handers (Fig. 4). One sample *t*-test for the dichotic condition revealed that N1 amplitude differences between the conditions were due to activation differences in superior temporal regions, which involved the planum temporale in the superior temporal gyrus (BA41/BA42) and the insula (BA13) in the left hemisphere.

3.5. Relationship between microstructural integrity and LD

For dichotic and noise conditions, we calculated Pearson's correlation coefficient between hemispheric LD in N1 peak onset and FA values of the posterior callosal third for the right-handers. Correlation analysis revealed a significant negative relation between FA and LD in dichotic condition ($r_{(102)} = -0.30$, $p < 0.01$, see Fig. 5). In contrast, no significant relation between FA value and LD was found in the noise condition ($r_{(102)} = -0.01$, $p = 0.93$).

Furthermore, we controlled for age as a potential confounding factor by computing a partial correlation between LD and FA of the posterior callosal third. The pattern of results remain stable as we found a significant negative correlation in the dichotic condition (partial $r_{(99)} = -0.32$, $p < 0.01$) and no significant correlation in the noise condition (partial $r_{(99)} = -0.01$, $p = 0.89$).

Since the observed association between hemispheric LD and FA value of the posterior callosal third might be confounded by the whole white matter FA, we performed a multiple regression analysis with LD of the dichotic condition as dependent variable and FA of the posterior third and whole white matter as predictors. Results indicate that only the FA of the posterior third provided unique contribution in predicting LD (beta = −0.32, $t_{(101)} = -2.37$, $p < 0.05$). The contribution of global white matter FA was not significant (beta = 0.03, $t_{(101)} = 0.22$, $p = 0.83$). Furthermore, in a second multiple regression we tested whether the association of LD and callosal microstructure was specific for callosal fibers located in the posterior third. Here we compute the regression analysis with LD of the dichotic condition as dependent variable and the FA of the three callosal segments (anterior third, mid segment, and posterior third) as predictors. Again only the FA values of the posterior third provided unique contribution in predicting LD (beta = −0.33, $t_{(101)} = -2.26$, $p < 0.05$; other predictors $p > 0.56$).

4. Discussion

To examine the role of microstructural callosal properties in combination with electrophysiological parameters for hemispheric latency differences in a lateralized cognitive task, we combined EEG measures in dichotic listening with DTI quantification of microstructural integrity of the corpus callosum. We performed separate analyses for our left- and right-handed subsamples, due to unequal numbers of participants per group, and focused on the bigger right-handed subsample. In right-handed participants, the early N1 latency was significantly faster in the left compared to the right hemisphere for the dichotic condition, but not for the noise condition. This is in accordance with previous studies (Eichele et al., 2005; Bayazit et al., 2009; Beste et al., 2015). As expected, sLORETA analyses indicate that the source of the N1 component is predominantly located in the left planum temporale. Furthermore, we found
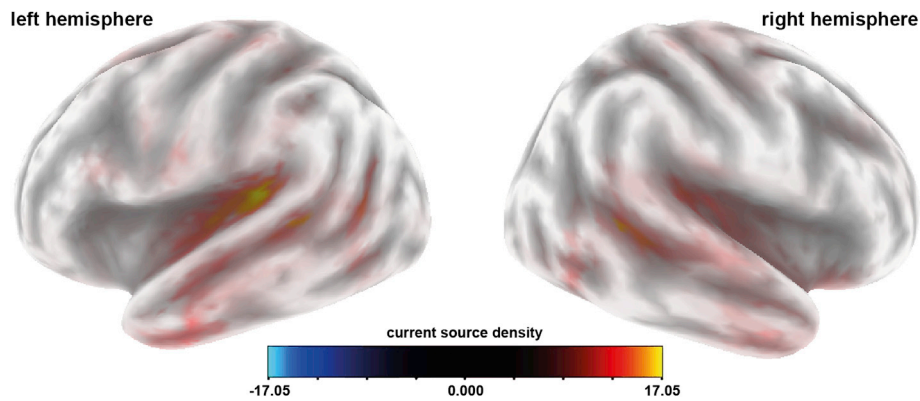
Fig. 4. Graphical representation of the sLORETA results showing cortical distribution of activation, which cause the N1 component in dichotic condition. Warm colors donating positive current source density, which reflect the source of the signal.
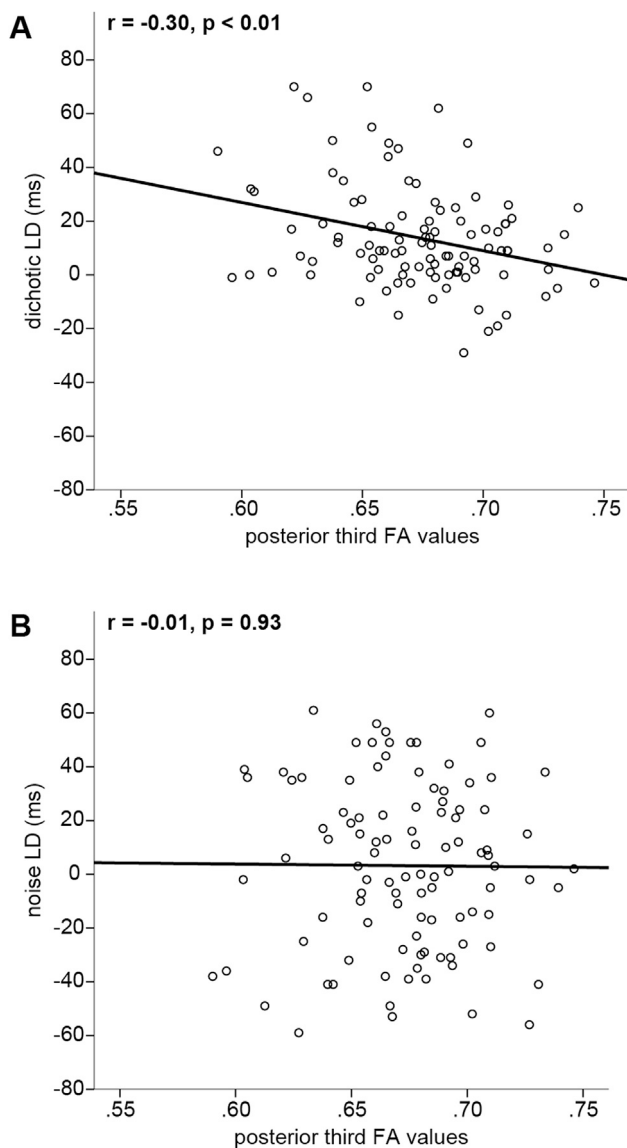
Fig. 5. Scatterplots showing the relationship between FA values of the posterior callosal third and latency differences (LD) in the dichotic condition (**A**) or noise condition (**B**).

that left-right latency difference in N1 amplitude for the dichotic and noise condition varied across individuals. Importantly, we found that the inter-individual variability of the left-right latency difference in N1

amplitudes was negatively correlated with the microstructure of the posterior third of the corpus callosum. This indicates that higher microstructural integrity of the corpus callosum leads to decreased hemispheric timing differences during dichotic listening.

This structure-function relationship is in accordance with the assumptions made by the theoretical models of dichotic listening (Kimura, 1967; Kinsbourne, 1970). While there is a direct link between electro-physiological hemispheric timing differences and behavioral outcome during DLT (Eichele et al., 2005), our results indicate that these electrophysiological timing differences are modulated by callosal microstructure. Previous studies suggested that decreased interhemispheric interaction is associated with greater functional hemispheric asymmetries (Yazgan et al., 1995; Gootjes et al., 2006; Westerhausen et al., 2006a), but callosal connections have often been evaluated in terms of size, hence only showing the relation on a macroscopic scale. Therefore, our study fills a crucial gap by showing the same association on a microstructural level.

More specifically, we focused on the posterior third of the corpus callosum, which consists of the isthmus and splenium (Hofer and Frahm, 2006). Previous studies suggest that callosal fibers in the isthmus (Cipolloni and Pandya, 1985; Park et al., 2008) and the splenium (Pollmann et al., 2002; Westerhausen et al., 2009) interconnect brain areas that are involved in processing speech information and auditory information in general. One important area, which is associated with hemispheric specialization for speech processing is the planum temporale (Josse and Tzourio-Mazoyer, 2004; Dorsaint-Pierre et al., 2006). With regards to the corpus callosum, microstructural analysis of the planum temporale showed that higher asymmetry in microcolumnar spacing is associated with fewer callosal projections (Chance et al., 2006). Importantly, the left planum temporale shows wider microcolumns and bigger interpatch distance between macrocolumns, which in turn, is thought to support the left hemisphere's superiority in processing temporal information (Hutsler and Galuske, 2003). As the analysis of temporal variation is crucial for understanding language (Shannon et al., 1995), the relatively higher temporal resolution of auditory cortices in the left hemisphere support its predominant role in speech perception (Zatorre et al., 2002).

Indeed, in our study the *sLORETA* analysis identified the left planum temporale and insula region as the source of the N1 component during the DLT. The insula is thought to play a role in coordinating anterior and posterior parts of the language system (Ardila et al., 2016). Importantly, the planum temporale shows activation during dichotic listening (Jancke and Shah, 2002) and is involved in stimulus selection during an auditory discrimination task in which participants attend to one ear while ignoring distracting stimuli to the other ear (Ross et al., 2010). In the present study, the left-right hemispheric timing difference for the dichotic and noise condition varied across individuals, but the structure-function relationship with callosal microstructure was only

found for the dichotic condition. Hence, the influence of callosal microstructure is specific for stimuli that trigger hemispheric bottom-up processing in an asymmetric fashion. This in turn strengthens the role of the corpus callosum as flexible and dynamic pathway, rather then a passive channel for automatic inter-hemispheric exchange (Westerhausen and Hugdahl, 2008).

The present study provides insight into the structure-function relation between functional laterality and callosal microstructure, measured as FA. However, FA is sensitive to many tissue properties (Beaulieu, 2009), including variation in myelin (Madler et al., 2008), axon diameter and axonal packing density (Takahashi et al., 2002). In a highly coherent tissue like the corpus callosum, the axon diameter hypothesis (Beaulieu, 2002; Genc et al., 2011a, b) would predict a positive correlation between FA values and latency difference, because increased axon diameter has been related to decreased FA (Barazany et al., 2009) and faster conduction velocities (Caminiti et al., 2009). Here a lower value of latency difference reflects faster conduction velocities across the hemispheres. However, the correlation between FA values and latency difference we found was negative, which does not support this hypothesis. An alternative explanation would be the myelin or axon packing density hypothesis, because increased myelin thickness as well as axon packing density hinder radial diffusion (Beaulieu, 2002), which in turn increases FA and is associated with faster nerve conduction velocity. Our data is in line with this hypothesis, because higher FA values in the posterior callosal third were associated with a lower latency difference. Hence, our study suggests that a variation in myelination or axon packing density might cause the observed interindividual variance in hemispheric latency difference.

Future studies could benefit from integrating complementary methods of white matter quantification like myelin water fraction (Laule et al., 2007; Madler et al., 2008) or neurite orientation dispersion and density imaging (NODDI (Zhang et al., 2012),) to investigate how these metrics influence inter-individual differences in functional brain asymmetries. Moreover, future studies could also benefit from integrating an assessment of genotypic variation in myelin-relevant genes (Ocklenburg et al., 2016b) in order to investigate the molecular basis of the results we observed in the present study. Furthermore, this study does not include possible asymmetric differences in subcortical auditory pathways, which might also contribute the onset of N1 latencies. Importantly, the here presented function-structure relationship could not be investigated in the left-handed subsample, because the missing difference in N1 peak onsets between conditions made the analyses of a function-structure relation obsolete. Reasons for the missing difference between conditions might be due to study limitations such as the small left-handed subsample size or the higher heterogeneity of left-handers in general (McManus, 2004). Therefore, future studies are needed to clarify the shown structure-function relation in a more homogeneous and bigger sample of left-handers.

In summary, the present study addressed an important gap in knowledge on the interrelation between inter-individual differences in microstructural integrity of the corpus callosum and hemispheric latency difference as a possible mechanism through which the corpus callosum mediates functional hemispheric asymmetries. The present study interrelates electrophysiology and the callosal microstructure in the context of asymmetric timing differences. Therefore, this study crucially contributes to the discussion about the role of the corpus callosum in functional laterality, by reintroducing the aspect of processing speed as a major factor for understanding functional hemispheric asymmetries.

Acknowledgements

Appendix A. Supplementary data

Supplementary data related to this article can be found at https://doi.org/10.1016/j.neuroimage.2017.09.048.

References

Aboitiz, F., Scheibel, A.B., Fisher, R.S., Zaidel, E., 1992. Fiber composition of the human corpus-callosum. Brain Res. 598 (1–2), 143–153. https://doi.org/10.1016/0006-8993(92)90178-c.

Ardila, A., Bernal, B., Rosselli, M., 2016. How localized are language brain Areas? A review of brodmann areas involvement in oral language. Archives Clin. Neuropsychol. 31 (1), 112–122. https://doi.org/10.1093/arclin/acv081.

Bamiou, D.E., Sisodiya, S., Musiek, F.E., Luxon, L.M., 2007. The role of the interhemispheric pathway in hearing. Brain Res. Rev. 56 (1), 170–182. https://doi.org/10.1016/j.brainresrev.2007.07.003.

Barazany, D., Basser, P.J., Assaf, Y., 2009. In vivo measurement of axon diameter distribution in the corpus callosum of rat brain. Brain 132, 1210–1220. https://doi.org/10.1093/brain/awp042.

Basser, P.J., Pierpaoli, C., 1996. Microstructural and physiological features of tissues elucidated by quantitative-diffusion-tensor MRI. J. Magn. Reson B 111 (3), 209–219.

Bayazit, O., Oniz, A., Hahn, C., Gunturkun, O., Ozgoren, M., 2009. Dichotic listening revisited: trial-by-trial ERP analyses reveal intra- and interhemispheric differences. Neuropsychologia 47 (2), 536–545. https://doi.org/10.1016/j.neuropsychologia.2008.10.002.

Beaulieu, C., 2002. The basis of anisotropic water diffusion in the nervous system - a technical review. NMR Biomed. 15 (7–8), 435–455. https://doi.org/10.1002/nbm.782.

Beaulieu, C., 2009. The Biological Basis of Diffusion Anisotropy. Diffusion MRI: from Quantitative Measurement to in Vivo Neuroanatomy, pp. 105–126.

Behrens, T.E.J., Berg, H.J., Jbabdi, S., Rushworth, M.F.S., Woolrich, M.W., 2007. Probabilistic diffusion tractography with multiple fibre orientations: what can we gain? Neuroimage 34 (1), 144–155. https://doi.org/10.1016/j.neuroimage.2006.09.018.

Beste, C., Heil, M., Domschke, K., Konrad, C., 2010. The relevance of the functional 5-HT1A receptor polymorphism for attention and working memory processes during mental rotation of characters. Neuropsychologia 48 (5), 1248–1254. https://doi.org/10.1016/j.neuropsychologia.2009.12.025.

Beste, C., Ocklenburg, S., von der Hagen, M., Di Donato, N., 2015. Mammalian cadherins DCHS1-FAT4 affect functional cerebral architecture. Brain Struct. Funct. https://doi.org/10.1007/s00429-015-1051-6.

Bethmann, A., Tempelmann, C., De Bleser, R., Scheich, H., Brechmann, A., 2007. Determining language laterality by fMRI and dichotic listening. Brain Res. 1133 (1), 145–157. https://doi.org/10.1016/j.brainres.2006.11.057.

Bloom, J.S., Hynd, G.W., 2005. The role of the corpus callosum in interhemispheric transfer of information: excitation or inhibition? Neuropsychol. Rev. 15 (2), 59–71. https://doi.org/10.1007/s11065-005-6252-y.

Bryden, M.P., Bulman-Fleming, M.B., 1994. Laterality effects in normal subjects - evidence for interhemispheric interactions. Behav. Brain Res. 64 (1–2), 119–129. https://doi.org/10.1016/0166-4328(94)90124-4.

Caminiti, R., Ghaziri, H., Galuske, R., Hof, P.R., Innocenti, G.M., 2009. Evolution amplified processing with temporally dispersed slow neuronal connectivity in primates. Proc. Natl. Acad. Sci. U. S. A. 106 (46), 19551–19556. https://doi.org/10.1073/pnas.0907655106.

Catani, M., Howard, R.J., Pajevic, S., Jones, D.K., 2002. Virtual in vivo interactive dissection of white matter fasciculi in the human brain. Neuroimage 17 (1), 77–94. https://doi.org/10.1006/nimg.2002.1136.

Chance, S.A., Casanova, M.F., Switala, A.E., Crow, T.J., 2006. Minicolumnar structure in Heschl's gyrus and planum temporale: asymmetries in relation to sex and callosal fiber number. Neuroscience 143 (4), 1041–1050. https://doi.org/10.1016/j.neuroscience.2006.08.057.

Cipolloni, P.B., Pandya, D.N., 1985. Topography and trajectories of commissural fibers of the superior temporal region in the rhesus-monkey. Exp. Brain Res. 57 (2), 381–389.

Clarke, J.M., Lufkin, R.B., Zaidel, F., 1993. Corpus-callosum morphometry and dichotic-listening performance - individual-differences in functional interhemispheric inhibition. Neuropsychologia 31 (6), 547–557. https://doi.org/10.1016/0028-3932(93)90051-Z.

Dale, A.M., Fischl, B., Sereno, M.I., 1999. Cortical surface-based analysis - I. Segmentation and surface reconstruction. Neuroimage 9 (2), 179–194. https://doi.org/10.1006/nimg.1998.0395.

Dippel, G., Beste, C., 2015. A causal role of the right inferior frontal cortex in implementing strategies for multi-component behaviour. Nat. Commun. 6 https://doi.org/10.1038/ncomms7587.

Dorsaint-Pierre, R., Penhune, V.B., Watkins, K.E., Neelin, P., Lerch, J.P., Bouffard, M., Zatorre, R.J., 2006. Asymmetries of the planum temporale and Heschl's gyrus: relationship to language lateralization. Brain 129, 1164–1176. https://doi.org/10.1093/brain/awl055.

Eichele, T., Nordby, H., Rimol, L.M., Hugdahl, K., 2005. Asymmetry of evoked potential latency to speech sounds predicts the ear advantage in dichotic listening. Cogn. Brain Res. 24 (3), 405–412. https://doi.org/10.1016/j.cogbrainres.2005.02.017.

Fields, R.D., 2008. White matter in learning, cognition and psychiatric disorders. Trends Neurosci. 31 (7), 361–370. https://doi.org/10.1016/j.tins.2008.04.001.

Fischl, B., Sereno, M.I., Dale, A.M., 1999. Cortical surface-based analysis - II: inflation, flattening, and a surface-based coordinate system. Neuroimage 9 (2), 195–207. https://doi.org/10.1006/nimg.1998.0396.

Foundas, A.L., Corey, D.M., Hurley, M.M., Heilman, K.M., 2006. Verbal dichotic listening in right and left-handed adults: laterality effects of directed attention. Cortex 42 (1), 79–86. https://doi.org/10.1016/S0010-9452(08)70324-1.

Gazzaniga, M.S., 2000. Cerebral specialization and interhemispheric communication - does the corpus callosum enable the human condition? Brain 123, 1293–1326. https://doi.org/10.1093/brain/123.7.1293.

Genc, E., Bergmann, J., Singer, W., Kohler, A., 2011a. Interhemispheric connections shape subjective experience of bistable motion. Curr. Biol. 21 (17), 1494–1499. https://doi.org/10.1016/j.cub.2011.08.003.

Genc, E., Bergmann, J., Tong, F., Blake, R., Singer, W., Kohler, A., 2011b. Callosal connections of primary visual cortex predict the spatial spreading of binocular rivalry across the visual hemifields. Front. Hum. Neurosci. 5, 161. https://doi.org/10.3389/fnhum.2011.00161.

Genc, E., Ocklenburg, S., Singer, W., Güntürkün, O., 2015. Abnormal interhemispheric motor interactions in patients with callosal agenesis. Behavioural Brain Research 293, 1–9.

Genc, E., Ocklenburg, S., Singer, W., & Güntürkün, O., Abnormal interhemispheric motor interactions in patients with callosal agenesis. Behavioural Brain Research, 293, 2015, 1-9 Gohil, K., Dippel, G., Beste, C., 2016. Questioning the role of the frontopolar cortex in multi-component behavior - a TMS/EEG study. Sci. Rep. 6 https://doi.org/10.1038/srep22317.

Gootjes, L., Bouma, A., Van Strien, J.W., Van Schijndel, R., Barkhof, F., Scheltens, P., 2006. Corpus callosum size correlates with asymmetric performance on a dichotic listening task in healthy aging but not in Alzheimer's disease. Neuropsychologia 44 (2), 208–217. https://doi.org/10.1016/j.neuropsychologia.2005.05.002.

Greenblatt, R.E., Ossadtchi, A., Pflieger, M.E., 2005. Local linear estimators for the bioelectromagnetic inverse problem. Ieee Trans. Signal Process. 53 (9), 3403–3412. https://doi.org/10.1109/Tsp.2005.853201.

Herrmann, C.S., Knight, R.T., 2001. Mechanisms of human attention: event-related potentials and oscillations. Neurosci. Biobehav. Rev. 25 (6), 465–476. https://doi.org/10.1016/S0149-7634(01)00027-6.

Herve, P.Y., Zago, L., Petit, L., Mazoyer, B., Tzourio-Mazoyer, N., 2013. Revisiting human hemispheric specialization with neuroimaging. Trends Cogn. Sci. 17 (2), 69–80. https://doi.org/10.1016/J.Tics.2012.12.004.

Hirnstein, M., Hugdahl, K., Hausmann, M., 2014. How brain asymmetry relates to performance - a large-scale dichotic listening study. Front. Psychol. 5 https://doi.org/10.3389/fpsyg.2014.00058.

Hiscock, M., Kinsbourne, M., 2011. Attention and the right-ear advantage: what is the connection? Brain Cogn. 76 (2), 263–275. https://doi.org/10.1016/j.bandc.2011.03.016.

Hofer, S., Frahm, J., 2006. Topography of the human corpus callosum revisited–comprehensive fiber tractography using diffusion tensor magnetic resonance imaging. Neuroimage 32 (3), 989–994. https://doi.org/10.1016/j.neuroimage.2006.05.044.

Horowitz, A., Barazany, D., Tavor, I., Bernstein, M., Yovel, G., Assaf, Y., 2015. In vivo correlation between axon diameter and conduction velocity in the human brain. Brain Struct. Funct. 220 (3), 1777–1788. https://doi.org/10.1007/s00429-014-0871-0.

Hugdahl, K., 2011. Fifty years of dichotic listening research - still going and going and introduction. Brain Cogn. 76 (2), 211–213. https://doi.org/10.1016/j.bandc.2011.03.006.

Hugdahl, K., Westerhausen, R., 2016. Speech processing asymmetry revealed by dichotic listening and functional brain imaging. Neuropsychologia 93, 466–481. https://doi.org/10.1016/j.neuropsychologia.2015.12.011.

Hutsler, J., Galuske, R.A.W., 2003. Hemispheric asymmetries in cerebral cortical networks. Trends Neurosci. 26 (8), 429–435. https://doi.org/10.1016/S0166-2236(03)00198-X.

Jancke, L., Shah, N.J., 2002. Does dichotic listening probe temporal lobe functions? Neurology 58 (5), 736–743.

Josse, G., Tzourio-Mazoyer, N., 2004. Hemispheric specialization for language. Brain Res. Rev. 44 (1), 1–12. https://doi.org/10.1016/j.brainresrev.2003.10.001.

Kimura, D., 1967. Functional asymmetry of the brain in dichotic listening. Cortex 3 (2), 163–178. https://doi.org/10.1016/s0010-9452(67)80010-8.

Kimura, D., 2011. From ear to brain. Brain Cogn. 76 (2), 214–217. https://doi.org/10.1016/j.bandc.2010.11.009.

Kinsbourne, M., 1970. The cerebral basis of lateral asymmetries in attention. Acta Psychol. (Amst) 33, 193–201.

Lamantia, A.S., Rakic, P., 1990. Cytological and quantitative characteristics of 4 cerebral commissures in the rhesus-monkey. J. Comp. Neurol. 291 (4), 520–537. https://doi.org/10.1002/cne.902910404.

Laule, C., Vavasour, I.M., Kolind, S.H., Li, D.K.B., Traboulsee, T.L., Moore, G.R.W., MacKay, A.L., 2007. Magnetic resonance imaging of myelin. Neurotherapeutics 4 (3), 460–484. https://doi.org/10.1016/j.nurt.2007.05.004.

Luders, E., Thompson, P.M., Toga, A.W., 2010. The development of the corpus callosum in the healthy human brain. J. Neurosci. 30 (33), 10985–10990. https://doi.org/10.1523/Jneurosci.5122-09.2010.

McManus, C., 2004. Right Hand, Left Hand: the Origins of Asymmetry in Brains, Bodies, Atoms and Cultures. Harvard University Press.

Madler, B., Drabycz, S.A., Kolind, S.H., Whittall, K.P., MacKay, A.L., 2008. Is diffusion anisotropy an accurate monitor of myelination? Correlation of multicomponent T2 relaxation and diffusion tensor anisotropy in human brain. Magn. Reson Imag. 26 (7), 874–888. https://doi.org/10.1016/j.mri.2008.01.047.

Mazziotta, J., Toga, A., Evans, A., Fox, P., Lancaster, J., Zilles, K., Mazoyer, B., 2001. A probabilistic atlas and reference system for the human brain: international Consortium for Brain Mapping (ICBM). Phil. Trans. R. Soc. B-Biol. Sci. 356 (1412), 1293–1322.

Mori, S., Zhang, J.Y., 2006. Principles of diffusion tensor imaging and its applications to basic neuroscience research. Neuron 51 (5), 527–539. https://doi.org/10.1016/j.neuron.2006.08.012.

Muckschel, M., Stock, A.K., Beste, C., 2014. Psychophysiological mechanisms of interindividual differences in goal activation modes during action cascading. Cereb. Cortex 24 (8), 2120–2129. https://doi.org/10.1093/cercor/bht066.

Mulert, C., Jager, L., Schmitt, R., Bussfeld, P., Pogarell, O., Moller, H.J., Hegerl, U., 2004. Integration of fMRI and simultaneous EEG: towards a comprehensive understanding of localization and time-course of brain activity in target detection. Neuroimage 22 (1), 83–94. https://doi.org/10.1016/j.neuroimage.2003.10.051.

Musiek, F.E., Weihing, J., 2011. Perspectives on dichotic listening and the corpus callosum. Brain Cogn. 76 (2), 225–232. https://doi.org/10.1016/j.bandc.2011.03.011.

Ocklenburg, S., Arning, L., Gerding, W.M., Epplen, J.T., Gunturkun, O., Beste, C., 2013a. FOXP2 variation modulates functional hemispheric asymmetries for speech perception. Brain Lang. 126 (3), 279–284. https://doi.org/10.1016/j.bandl.2013.07.001.

Ocklenburg, S., Friedrich, P., Güntürkün, O., Genc, E., 2016a. Intrahemispheric white matter asymmetries: the missing link between brain structure and functional lateralization? Rev. Neurosci. 27 (5), 465–480. https://doi.org/10.1515/revneuro-2015-0052.

Ocklenburg, S., Gerding, W.M., Arning, L., Genc, E., Epplen, J.T., Gunturkun, O., Beste, C., 2016b. Myelin genes and the corpus callosum: proteolipid protein 1 (PLP1) and contactin 1 (CNTN1) gene variation modulates interhemispheric integration. Mol. Neurobiol. https://doi.org/10.1007/s12035-016-0285-5.

Ocklenburg, S., Gunturkun, O., Beste, C., 2012. Hemispheric asymmetries and cognitive flexibility: an ERP and sLORETA study. Brain Cogn. 78 (2), 148–155. https://doi.org/10.1016/j.bandc.2011.11.001.

Ocklenburg, S., Hugdahl, K., Westerhausen, R., 2013b. Structural white matter asymmetries in relation to functional asymmetries during speech perception and production. Neuroimage 83, 1088–1097. https://doi.org/10.1016/j.neuroimage.2013.07.076.

Olbrich, S., Mulert, C., Karch, S., Trenner, M., Leicht, G., Pogarell, O., Hegerl, U., 2009. EEG-vigilance and BOLD effect during simultaneous EEG/fMRI measurement. Neuroimage 45 (2), 319–332. https://doi.org/10.1016/j.neuroimage.2008.11.014.

Oldfield, R.C., 1971. The assessment and analysis of handedness: the Edinburgh inventory. Neuropsychologia 9 (1), 97–113.

Park, H.J., Kim, J.J., Lee, S.K., Seok, J.H., Chun, J., Kim, D.I., Lee, J.D., 2008. Corpus callosal connection mapping using cortical gray matter parcellation and DT-MRI. Hum. Brain Mapp. 29 (5), 503–516. https://doi.org/10.1002/hbm.20314.

Pascual-Marqui, R.D., 2002. Standardized low-resolution brain electromagnetic tomography (sLORETA): technical details. Meth. Find. Exp. Clin. Pharmacol. 24, 5–12.

Pascual-Marqui, R.D., Michel, C.M., Lehmann, D., 1994. Low resolution electromagnetic tomography: a new method for localizing electrical activity in the brain. Int. J. Psychophysiol. 18 (1), 49–65.

Peru, A., Beltramello, A., Moro, V., Sattibaldi, L., Berlucchi, G., 2003. Temporary and permanent signs of interhemispheric disconnection after traumatic brain injury. Pii S0028-3932(02)00203-8 Neuropsychologia 41 (5), 634–643. https://doi.org/10.1016/S0028-3932(02)00203-8.

Pollmann, S., Maertens, M., von Cramon, D.Y., Lepsien, J., Hugdahl, K., 2002. Dichotic listening in patients with splenial and nonsplenial callosal lesions. Neuropsychology 16 (1), 56–64. https://doi.org/10.1037/0894-4105.16.1.56.

Ringo, J.L., Doty, R.W., Demeter, S., Simard, P.Y., 1994. Time is of the essence - a conjecture that hemispheric-specialization arises from interhemispheric conduction delay. Cereb. Cortex 4 (4), 331–343. https://doi.org/10.1093/Cercor/4.4.331.

Ross, B., Hillyard, S.A., Picton, T.W., 2010. Temporal dynamics of selective attention during dichotic listening. Cereb. Cortex 20 (6), 1360–1371. https://doi.org/10.1093/cercor/bhp201.

Sammler, D., Kotz, S.A., Eckstein, K., Ott, D.V.M., Friederici, A.D., 2010. Prosody meets syntax: the role of the corpus callosum. Brain 133, 2643–2655. https://doi.org/10.1093/brain/awq231.

Schulte, T., Sullivan, E.V., Muller-Oehring, E.M., Adalsteinsson, E., Pfefferbaum, A., 2005. Corpus callosal microstructural integrity influences interhemispheric processing: a diffusion tensor imaging study. Cereb. Cortex 15 (9), 1384–1392. https://doi.org/10.1093/cercor/bhi020.

Sekihara, K., Sahani, M., Nagarajan, S.S., 2005. Localization bias and spatial resolution of adaptive and non-adaptive spatial filters for MEG source reconstruction. Neuroimage 25 (4), 1056–1067. https://doi.org/10.1016/j.neuroimage.2004.11.051.

Shannon, R.V., Zeng, F.G., Kamath, V., Wygonski, J., Ekelid, M., 1995. Speech recognition with primarily temporal cues. Science 270 (5234), 303–304. https://doi.org/10.1126/science.270.5234.303.

Takahashi, M., Hackney, D.B., Zhang, G.X., Wehrli, S.L., Wright, A.C., O'Brien, W.T., Selzer, M.E., 2002. Magnetic resonance microimaging of intraaxonal water diffusion in live excised lamprey spinal cord. Proc. Natl. Acad. Sci. U. S. A. 99 (25), 16192–16196. https://doi.org/10.1073/pnas.252249999.

Van der Haegen, L., Westerhausen, R., Hugdahl, K., Brysbaert, M., 2013. Speech dominance is a better predictor of functional brain asymmetry than handedness: a combined fMRI word generation and behavioral dichotic listening study. Neuropsychologia 51 (1), 91–97. https://doi.org/10.1016/j.neuropsychologia.2012.11.002.

Van Schependom, J., Gielen, J., Laton, J., Sotiropoulos, G., Vanbinst, A.M., De Mey, J., Nagels, G., 2017. The effect of morphological and microstructural integrity of the corpus callosum on cognition, fatigue and depression in mildly disabled MS patients. Magn. Reson. Imag. 40, 109–114. https://doi.org/10.1016/j.mri.2017.04.010.

Wedeen, V.J., Hagmann, P., Tseng, W.Y.I., Reese, T.G., Weisskoff, R.M., 2005. Mapping complex tissue architecture with diffusion spectrum magnetic resonance imaging. Magn. Reson. Med. 54 (6), 1377–1386. https://doi.org/10.1002/mrm.20642.

Westerhausen, R., Gruner, R., Specht, K., Hugdahl, K., 2009. Functional relevance of interindividual differences in temporal lobe callosal pathways: a DTI tractography study. Cereb. Cortex 19 (6), 1322–1329. https://doi.org/10.1093/cercor/bhn173.

Westerhausen, R., Hugdahl, K., 2008. The corpus callosum in dichotic listening studies of hemispheric asymmetry: a review of clinical and experimental evidence. Neurosci. Biobehav. Rev. 32 (5), 1044–1054. https://doi.org/10.1016/J.Neubiorev.2008.04.005.

Westerhausen, R., Kreuder, F., Huster, R.J., Smit, C.M., Woerner, W., Schweiger, E., Wittling, W., 2006a. Is interhemispheric transfer time associated with macro- and microstructure of the Corpus callosum? J. Psychophysiol. 20 (2), 147–147.

Westerhausen, R., Kreuder, F., Woerner, W., Huster, R.J., Smit, C.M., Schweiger, E., Wittling, W., 2006b. Interhemispheric transfer time and structural properties of the corpus callosum. Neurosci. Lett. 409 (2), 140–145. https://doi.org/10.1016/j.neulet.2006.09.028.

Westerhausen, R., Woerner, W., Kreuder, F., Schweiger, E., Hugdahl, K., Wittling, W., 2006c. The role of the corpus callosum in dichotic listening: a combined morphological and diffusion tensor imaging study. Neuropsychology 20 (3), 272–279. https://doi.org/10.1037/0894-4105.20.3.272.

Yazgan, M.Y., Wexler, B.E., Kinsbourne, M., Peterson, B., Leckman, J.F., 1995. Functional-significance of individual variations in callosal area. Neuropsychologia 33 (6), 769–779. https://doi.org/10.1016/0028-3932(95)00018-X.

Zarei, M., Johansen-Berg, H., Smith, S., Ciccarelli, O., Thompson, A.J., Matthews, P.M., 2006. Functional anatomy of interhemispheric cortical connections in the human brain. J. Anat. 209 (3), 311–320. https://doi.org/10.1111/j.1469-7580.2006.00615.x.

Zatorre, R.J., Belin, P., Penhune, V.B., 2002. Structure and function of auditory cortex: music and speech. Trends Cogn. Sci. 6 (1), 37–46. https://doi.org/10.1016/S1364-6613(00)01816-7.

Zatorre, R.J., Fields, R.D., Johansen-Berg, H., 2012. Plasticity in gray and white: neuroimaging changes in brain structure during learning. Nat. Neurosci. 15 (4), 528–536. https://doi.org/10.1038/nn.3045.

Zhang, H., Schneider, T., Wheeler-Kingshott, C.A., Alexander, D.C., 2012. NODDI: practical in vivo neurite orientation dispersion and density imaging of the human brain. Neuroimage 61 (4), 1000–1016. https://doi.org/10.1016/j.neuroimage.2012.03.072.